

Equilibrium and Kinetic Studies of Safranin Adsorption on Alkali-Treated Mango Seed Integuments

Mohamad Rasool Malekbala, Salman Masoudi Soltani, Sara Kazemi Yazdi, and Soraya Hosseini

Abstract—In this study, Safranin absorption onto mango seed integuments (raw and NaOH treated) has been investigated. The effects of solution pH, initial dye concentration, contact time, point zero charge and surface chemistry of the adsorbent were studied batch-wise. Safranin adsorption onto the untreated sample is influenced by the pH of the aqueous solution whereas, adsorption with the NaOH-treated sample is independent of the pH of the solution. Boehm titration showed the acidic groups of the treated sample has a higher value (0.660 mmol/g) than the untreated sample (0.375 mmol/g). Freundlich isotherm model resulted in the best data fitting for the untreated sample. However, Langmuir model indicated the best fitting with the NaOH-treated sample. The adsorption kinetics was found to obey pseudo second order kinetic model for both samples. An approximate increase of 26 % was found in the amount of dye adsorption due to the treatment with NaOH.

Index Terms—Adsorption, mango seed integument, safranin, NaOH treatment.

I. INTRODUCTION

Wastewaters generated by many industries such as textile, leather tanning, paper, pulp, rubbers, cosmetic and food are known as the most consumer dyes and pigments. Most of dyes are carcinogenic and mutagenic due to the presence and involvement of hazardous chemicals in their synthesis' processes. Hence, dye removal from such wastewaters is known as one of the major environmental problems [1]. There are currently numerous treatment processes for such wastewaters due to the presence of dyes; amongst which we can mention biodegradation [2], chemical oxidation [3], foam flotation [4], electrolysis [5], adsorption [6], chemical coagulation [7] and photocatalysis [8]. Nevertheless, adsorption processes provide an effective alternative treatment approach for dye removal due to the lower initial cost, sludge free clean, flexibility and simplicity of design, simple operation, easy recovery and insensitivity to toxic pollutants [9].

Since most agricultural solid wastes are inexpensive, abundant and easily available, consequently many researchers have focused on the feasibility of low-cost materials that were derived from agricultural wastes for the removal of various dyes, heavy metals and other pollutants. Wastes or by-products of industries can be used directly or after some treatments as adsorbents in adsorption processes.

The most commonly studied agricultural-based wastes used as adsorbents include rice husk [10], wood sawdust [11]; pine sawdust [12]; corncob [13], sunflower stalk [14]; bagasse [15], durian shell [16]. Mango seed kernel has been studied as an adsorbent for the removal of methylene blue from its aqueous solutions [17]. A massive amount of mango solid waste is currently produced by juice and food industries. The present study is an attempt to investigate the possibility of using mango seeds integument and its treatment procedure with NaOH to remove safranin as a cationic dye from aqueous solutions.

Safarnine O (Basic Red2) a contaminant agent has widely been used in food, textile, histology, cytology, bacteriology and some other industries. Two types of samples are considered in order to study safranin adsorption, namely mango seed integument (untreated) and the treated sample with NaOH (treated mango seed). To study the influencing operational parameters, variables such as the pH of the solution, initial dye concentration, point zero charge, surface chemistry of adsorbent and contact time were closely studied.

II. MATERIALS AND METHODS

A. Preparation and Characterization of Adsorbent

The solid wastes samples were collected and their integuments were removed manually from the seeds. The integuments were used in order to study of safranin adsorption. In the present study, the raw integuments (untreated) and its immersion in NaOH (treated) were studied individually, as the potential adsorbents. The integuments were washed with distilled water and then immersed in an HCL solution (0.01 N) to remove impurities for 24 h. They were then rinsed with distilled water. Next, the samples were dried in an oven at 70 °C for 48 h to reach a constant weight. To powder the matters, the dried samples were chopped and then ground using a blender. The powders were then screened in a sieve with a nominal size of 110 µm and labeled as the untreated sample.

The dried samples were next chemically activated by the immersion into NaOH solution (1N) for 24 h, assuming that all bases were incorporated with the integument. After that, the samples were rinsed with distilled water and then dried in an oven at 70 °C for 48 h to reach a constant weight. The surface chemistry of the samples was estimated by Boehm titration method. The functional groups of the surface of the samples were investigated by Fourier Transform Infrared (Perkin Elmer, Norwalk) analysis, ranging from 4000 to 400 cm⁻¹. The dye solution concentration was measured by a UV-visible spectrophotometer (Ultrospec 6300 pro) at the maximum adsorption wavelength.

Manuscript received May 16, 2012; revised June 7, 2012.

The authors are with the the department of chemical and environmental engineering, Universiti Putra Malaysia 43400 UPM Serdang Selangor, Malaysia (e-mail: m.r.malekbala@gmail.com, soraya@eng.ukm.my, keyx1smt@nottingham.edu.my, sara.yazdi@nottingham.edu.my).

B. Adsorbate

Cationic dye (safranin O, C.I. 50240, 350.85 gmol^{-1} , $\text{C}_{20}\text{H}_{19}\text{N}_4\text{Cl}$) as the pollutant (95% purity), was used without further purification. An accurately weighed quantity of safranin was dissolved in 1 liter of distilled water in order to prepare the stock solution (1000 mg/l). Experimental solutions of the desired concentrations were prepared by the dilution of the stock solution. The residual dye concentration was estimated by the determination of the dye absorbance using UV/vis spectrophotometer at $\lambda_{\text{max}} = 516 \text{ nm}$. The chemical structure of safranin is shown in Fig. 1.

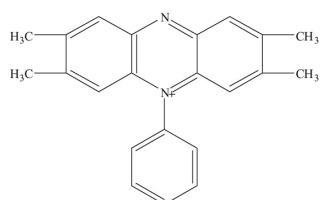


Fig. 1. Chemical structure of safranin

C. Determination of Point Zero Charge, Effect of pH and Surface Chemistry

The point zero charge of adsorbent was estimated by solid addition method [18]. Batch equilibrium method was used for determining variables such as point zero charge, pH effect and surface chemistry. The activation of acidic or basic functional groups of adsorbents approaches zero at point of zero charge (pH_{pzc}). To determine the point of zero charge, 1 g of each sample was added to conical flasks containing 50 ml of KNO_3 solution (0.01 N) and the initial pH was adjusted to be between 2 to 11 using KOH (0.01 N) and HNO_3 (0.01) solutions. The conical flasks were sealed and shaken vigorously for 48 h. The mixture was filtered and the pH of the solution was measured in order to calculate the final pH. The intersection point of the obtained curve indicated the amount of point zero charge.

The amount of adsorption may depend on the pH of the solution due to the adsorption process in the aqueous solution. The pH of the solution is affected by the surface charge of the adsorbent, the degree of ionization of the adsorbent in the solution and the dissociation of functional groups on the surface of the adsorbent [19]. The pH effect was studied by varying the initial pH in a range of 2 to 10 under constant process parameters and the initial concentration of 100 mg/L at equilibrium conditions. 1g of the adsorbent was added to each conical flask containing 250 ml dye solution. The conical flasks were constantly shaken in a shaker at 200 rpm for 48 h. The maximum amount of adsorption was calculated by the determination of the residual concentration of the solution.

The amount of acidity/basicity of functional groups was determined by Boehm titration method [20]. A known amount of adsorbent was added into 50 ml of the solutions of NaHCO_3 (0.1 N), Na_2CO_3 (0.1 N), NaOH (0.1 N) and HCl (0.1 N). The conical flasks were sealed and shaken at room temperature for 48 h. The solutions were then filtered and 10 ml of each filtrate was titrated with HCl (0.1 N) and NaOH (0.1 N). The acidic strength was calculated by measuring the volume of HCl consumed due to the titration with the solutions of NaOH , Na_2CO_3 and NaHCO_3 . Accordingly, the basic strength was calculated by measuring

the volume of NaOH consumed in order to neutralize HCl .

D. Safranin Adsorption

Adsorption capacities, kinetics and isothermal experiments were all carried out in the batch mode at the maximum pH and by varying the initial concentrations of dye in the aqueous solution (50 to 300 mg/L). Safranin adsorption experiments were performed by shaking a series of conical flasks containing 250 ml the different initial concentrations of dye solution in a shaker at 200 rpm. Studies were conducted at different time intervals of 15th, 30th and 60th minutes to reach the adsorption equilibrium and the determination of the maximum safranin removal. Due to the pH drop in the aqueous solution, the pH of the solution was continuously controlled and adjusted using NaOH (0.1 N) in order to maintain a constant pH of 10. The mixture was then separated by means of a centrifuge operating at 5000 rpm for 5 min to measure the supernatant concentration. The supernatant concentrations were calculated by measuring the absorbance at the maximum wavelengths of dye at $\lambda = 516 \text{ nm}$. The amount of dye adsorbed by the adsorbent was calculated using the following equation:

$$q_t = \frac{(C_0 - C_t)V}{m} \quad (1)$$

where C_0 and C_t (mg/L) are the concentrations of dye at the beginning and time (t) of the experiment, respectively, V is the volume of the solution (l) and m is the mass of adsorbent (g).

E. Safranin Desorption

Batch systems were used in the desorption processes in order to evaluate the regeneration efficiency. The dye-loaded adsorbent (~1g) was added to conical flasks containing 250 ml HCl (0.5M) aqueous solution and stirring at 200 rpm for 24 h. The mixture was filtrated and the supernatant concentration was subsequently measured by UV absorbance.

III. RESULTS AND DISCUSSIONS

A. Characterization of Adsorbents

Boehm titration method was used to characterize the surface chemistry of the adsorbents. The surface acidity was measured based on the assumption of Boehm method which states that carboxyl, lactone and phenolic groups are neutralized by NaOH , NaHCO_3 and Na_2CO_3 solutions. The surface basicity was estimated by neutralization using HCl solution. The physicochemical properties of adsorbents are listed in Table I.

The treated sample shows the concentration of acidic groups (0.660 mmol/g) which is greater than that of the untreated (0.3740 mmol/g). The untreated case reveals higher basic sites (0.0233 mmol/g) compared to the treated one (0.0123 mmol/g). The NaOH treatment showed an increase in phenolics formation approximately three times more than the untreated sample while carboxyl and lactone groups were unchanged. The phenolic groups contribute to the electron-acceptor characteristics of the aromatic ring of

safranin [21].

TABLE I: THE BOEHM RESULTS FOR THE TWO SAMPLES

Untreated		Treated	
	0.1533		0.1519
Carboxylic (mmol/g)	0.1157	Carboxylic (mmol/g)	0.1207
Lactonic (mmol/g)		Lactonic (mmol/g)	
Phenolic (mmol/g)	0.1059	Phenolic (mmol/g)	0.3874
Acidity (mmol/g)		Acidity (mmol/g)	
Basicity (mmol/g)	0.3750	Basicity (mmol/g)	0.6600
	0.0233		0.0123

The FTIR spectrum of samples indicated weak and broad peaks in the region of $3840 - 600 \text{ cm}^{-1}$ as shown in Fig. 2. The FTIR bands can be assigned to the presence of carboxyls, lactones, and phenols groups as reported by the surface chemistry analysis using Boehm method. FTIR spectrum of the treated and untreated mango seed integument indicated the strong peak of hydroxyl (O-H) group at wave number 3350 cm^{-1} . The absorption bands around 2920 cm^{-1} corresponds to CH_3 (alkane group). The carboxyl groups show two main absorption features corresponding to a carbonyl (C=O) at 1734 cm^{-1} stretching vibrations in ketones, aldehydes, lactones and carboxylic groups and C-OH vibrations in the range of 1200 to 1300 cm^{-1} . The band of alkenyl C=C stretch was assigned at 1640 cm^{-1} . The band 1427 cm^{-1} is probably due to amides functional groups of primary amides and aliphatic amides [22]. The vibration of band 600 cm^{-1} was attributed to aromatic C-H bending. The integument of mango seed is mainly composed by cellulose, lignin and hemicelluloses. The treatment of mango seed integument by NaOH shows the high lignin content in mango seed after NaOH treatment, consequently producing cellulose acetate ($\text{C}_6\text{H}_{10}\text{O}_5$) [23].

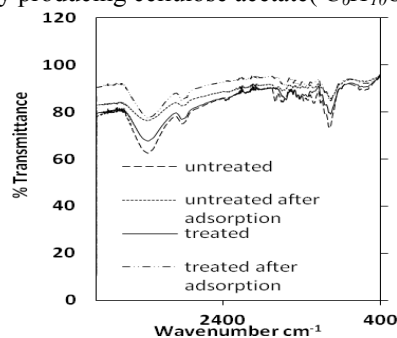
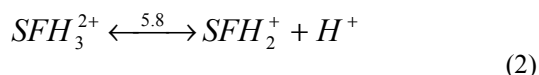


Fig. 2. FTIR pattern of the samples before and after absorption in range of $4000-400 \text{ cm}^{-1}$.

B. Effect of pH

Safranin molecules ($\text{pK}_a=5.8$) can be reformed to fully protonated as in highly acidic solutions and deprotonated at high pH [24]. The dye molecules show a high positive charge density at a lower pH as follows.



The pH effect was studied by varying the initial dye concentrations to obtain the highest degree of safranin removal. The untreated sample demonstrated the high

adsorption at the high pH (~ 10) compared to low pH , whereas the variation of pH is not effective in the treated sample. As seen in Fig. 3, the pH effect revealed different behavior for the treated and the untreated samples. When the pH of the solution increased from 3 to 5, the amount of adsorbed sharply increased as well. Upon a further increase in pH from 5 to 10, the adsorption slightly increases and was found to reach its maximum value at pH 10 in the untreated sample. The pH_{pzc} was found be 8.30, therefore at $\text{pH} > 8.30$ the surface charge is negative, favoring the cations adsorption while anions adsorption is enhanced at $\text{pH} < 8.30$.

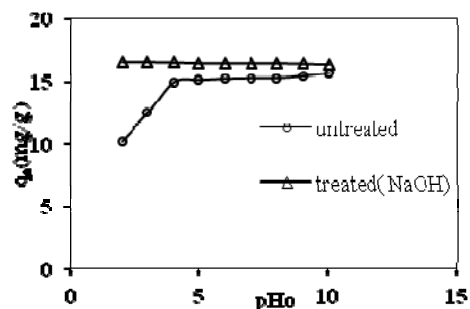


Fig. 3. Effect of pH on safranin adsorption using mango seed integument ($C_0=100 \text{ mg/L}$).

The treated sample shows no obvious effect on the safranin removal efficiency by increasing pH from 2 to 10. This is seen by the negligible difference of adsorption obtained when pH was changed in the mentioned range. No significant effect on the adsorption of safranin was revealed under alkaline condition by changing the initial pH ; therefore both samples were conducted at pH 10. Also, the point zero charge (pH_{pzc}) was not detected in the pH range as seen in Fig. 4.

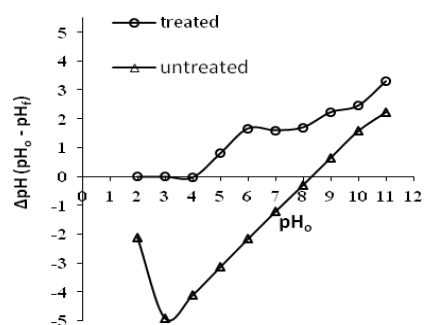


Fig. 4. Point of zero charge (pH_{pzc}) of two adsorbents using KNO_3 .

C. Effect of Contact Time and Initial Concentration

Fig. 5 (a) and (b) show the effects of contact time and initial concentration on the safranin adsorption. Dye removal is rapid at the initial stages of adsorption at different initial concentration values. By increasing the contact time, the adsorption gradually decreases until the equilibrium is finally reached. As the pH dropped in safranin aqueous solution, the pH of the solution was kept constant at 10 by adding NaOH solution (0.5 M) After 400 min of the adsorption process, equilibrium in dye adsorption was achieved. If the initial dye concentration is higher, equilibrium is reached at some longer time. It was found that an increase in the initial dye concentration led to an increased dye uptake. The Adsorption kinetics and equilibrium isotherms were analyzed by the dye uptake at different time intervals of 15th and 60th minutes. The

adsorption capacity was found to be 31 mg/g for the untreated sample, whereas the value of 42 mg/g was measured for the untreated sample. The NaOH treatment increased the dye uptake by approximately 26 % compared to the untreated sample.

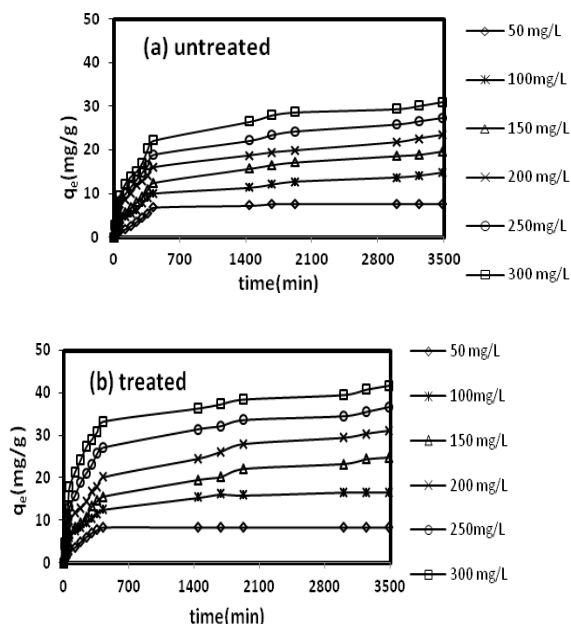


Fig. 5. Effect of contact time on adsorption safranin for various initial concentrations (a) untreated sample, (b) treated sample.

D. Adsorption Isotherm

The adsorption isotherms were obtained in sufficient time of 400 min at different initial concentrations of 50 to 300 mg/g. The equilibrium data were modeled by the two common models of Freundlich and Langmuir. The Langmuir model is expressed based on the assumptions of monolayer adsorption onto adsorbent surface, finite capacity adsorption for adsorbate and the occupation of a dye molecule on one site [25]. The Langmuir is represented as follow:

$$\frac{C_e}{q_e} = \frac{1}{q_m k_L} + \frac{C_e}{q_m} \quad (3)$$

where q_m and k_L are the maximum amount of dye per unit of the mass of the adsorbent to form a complete monolayer on the surface (mg/g) and Langmuir constant (L/mg), respectively. The plot of C_e/q_e versus C_e demonstrates a straight line of which the slope and intercept represent q_m and k_L , respectively. Freundlich empirical equation has been used to describe heterogeneous systems taking into account the interactions between adsorbed molecules. The equation is expressed as follows [26]:

$$\text{Log} q_e = \text{Log} k_F + \frac{1}{n} \text{log} C_e \quad (4)$$

where k_F and $1/n$ are Freundlich constants, representing the bonding energy and heterogeneity factor, respectively. k_F and $1/n$ can be estimated by the intercept and slope of the plot of $\text{log} q_e$ versus $\text{log} C_e$. The Langmuir and Freundlich parameters are listed in Table II.

TABLE II: ISOTHERM PARAMETERS OF THE TWO MODELS (LANGMUIR & FREUNDLICH)

Untreated		Treated	
Langmuir		Langmuir	
k_L (L/g)	13.62	k_L (L/g)	23.30
q_m (mg/g)	34.48	q_m (mg/g)	43.47
r^2	0.971	r^2	0.996
Freundlich		Freundlich	
k_F (mg/g)	5.088	k_F (mg/g)	18.70
$1/n$	0.383	$1/n$	0.251
r^2	0.978	r^2	0.956

The adsorption capacities of the two models were compared to the experimental data as shown in Fig. 6 (a) and (b). Obviously, the Freundlich model was the best fit isotherm for the untreated sample since it has the higher value of correlation coefficient R^2 (0.978) in comparison with Langmuir model (0.971). In the treated sample as shown in Fig. 6(b), the Langmuir model was found to best fit the adsorption isotherm data with the higher value of R^2 (0.996) as compared to Freundlich model (0.956).

The essential characteristics of Langmuir equation can be expressed as a dimensionless group named R_L , as follows:

$$R_L = \frac{1}{1 + k_L C_0} \quad (5)$$

Isotherm type can be evaluated by determining the R_L value as to be irreversible ($R_L = 0$), favorable ($0 < R_L < 1$), linear ($R_L = 1$) and unfavorable ($R_L > 1$) [27]. The values of R_L were found to be in the range of 0.996 - 0.507 and represent favorable adsorption.

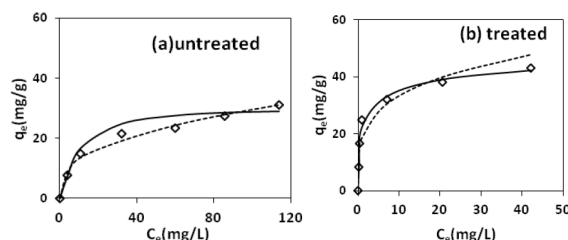


Fig. 6. A comparison between the obtained isotherms data with the experimental data: (a) the untreated sample, (b) the treated sample.

E. Kinetic Studies

In order to investigate the kinetics of the process, three models of pseudo-first-order, second-order and intraparticle diffusion were all fitted to the experiments data. Pseudo-first-order and second-order equations are described by Lagrangren [28] and Ho [29], respectively. The possibility of intra-particle diffusion was explored by Webber and Morris equation [30]. The linearised forms of the pseudo-first-order and pseudo-second-order and intraparticle diffusion models were given in Equation (6), (7) and (8), respectively.

$$\text{log}(q_e - q_t) = \text{log} q_e - \frac{k_1 t}{2.303} \quad (6)$$

The pseudo-first-order rate constant, k_1 and $q_{e,cal}$ are calculated using the slope and intercept of the plot $\text{log}(q_e - q_t)$ versus t .

$$\frac{t}{q_t} = \frac{1}{k_2 q_e^2} + \frac{t}{q_e} \quad (7)$$

The pseudo second-order rate constant k_2 and $q_{e,cal}$ can be obtained from the intercept and slope of the plot of t/q_t versus t .

$$q_t = k_i t^{1/2} + I \quad (8)$$

where k_i and I are the diffusion rate constant ($\text{mg/g min}^{1/2}$) and intercept that were estimated from the linear plot of q_t versus $t^{1/2}$.

TABLE III: KINETICS PARAMETERS OF SAFRANINE ADSORPTION ONTO SEED INTEGUMENT WITH PSEUDO FIRST (A) AND SECOND ORDER (B) MODELS

(a)				
C_0	$q_{e,exp}$	$q_{e,cal}$	$K_1 * 10^{-4}$	R^2
mg/L	(mg/g)	(mg/g)	min^{-1}	
50	7.6900	7.9983	23	0.958
100	14.844	13.489	2.53	0.968
150	21.639	17.906	2.56	0.986
200	23.362	19.678	2.76	0.961
250	27.407	23.442	2.99	0.970
300	31.923	26.363	3.22	0.960

(b)				
C_0	$q_{e,exp}$	$q_{e,cal}$	$K_1 * 10^{-4}$	R^2
mg/L	(mg/g)	(mg/g)	min^{-1}	
50	7.6900	7.9983	23	0.958
100	14.844	13.489	2.53	0.968
150	21.639	17.906	2.56	0.986
200	23.362	19.678	2.76	0.961
250	27.407	23.442	2.99	0.970
300	31.923	26.363	3.22	0.960

TABLE IV: KINETICS PARAMETERS OF SAFRANINE ADSORPTION ONTO ALKALI-TREATED MANGO SEED INTEGUMENT WITH PSEUDO FIRST (A) AND SECOND ORDER (B) MODELS

(a)				
C_0	$q_{e,exp}$	$q_{e,cal}$	$K_1 * 10^{-4}$	R^2
mg/L	(mg/g)	(mg/g)	min^{-1}	
50	8.3265	9.2469	69	0.958
100	16.613	13.803	23	0.960
150	24.839	21.877	2.3	0.979
200	32.154	25.644	2.5	0.951
250	38.236	30.619	2.5	0.972
300	42.977	32.960	2.8	0.957

(b)				
C_0	$q_{e,exp}$	$q_{e,cal}$	$K_2 * 10^{-4}$	R^2
mg/L	(mg/g)	(mg/g)	g/mg.min	
50	8.3265	8.6956	10	0.997
100	16.613	17.543	3.8	0.998
150	24.839	25.641	1.7	0.991
200	32.154	32.258	1.5	0.992
250	38.236	37.037	1.1	0.997
300	42.977	43.478	0.9	0.997

The comparison was carried out based on the higher value r^2 and well agreement between $q_{e,cal}$ and $q_{e,exp}$ for two models pseudo first-order and pseudo second-order. The best model was selected by considering two assumptions. All derived kinetic parameters of first-order and second order models are listed in Table III and IV.

The kinetics data are matched to the initial stage (400 min) of the adsorption process using first-order model and the whole range of experimental data was not fitted with the model as shown in Fig. 7. Thus, the pseudo-first-order model does not obey to the experimental data. The significant discrepancy was found between $q_{e,cal}$ and $q_{e,exp}$. The obtained results suggested the adsorption may not be diffusion controlled [19].

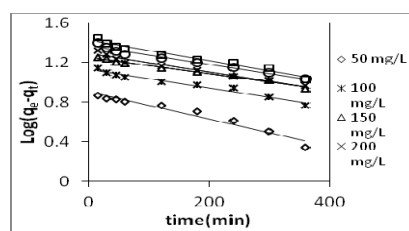


Fig. 7. Pseudo-first-order kinetics of safranine adsorption onto the treated sample at different initial dye concentrations.

The kinetics data were well represented for whole range of contact time in all concentrations with the second-order model as shown in Fig. 8. Safranine adsorption was found to follow the pseudo second-order kinetic with well agreement between $q_{e,cal}$ and $q_{e,exp}$ and high values of the correlation coefficient, ($R^2 > 0.997$). Due to obey the pseudo second-order kinetic model for the entire adsorption, the adsorption may obey chemisorptions [19]. It was found that the rate constant, k_2 , decreased from $10 \times 10^{-4} \text{ min}^{-1}$ to $0.9 \times 10^{-4} \text{ min}^{-1}$ for initial concentrations of safranine range in the range 50 to 300 mg/L.

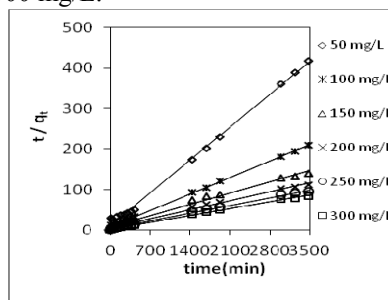


Fig. 8. Pseudo-second-order kinetics of safranine adsorption onto the treated sample at different initial dye concentrations.

Fig. 9 represented the plot q_t versus $t^{1/2}$ for the initial concentrations in ranging 50 to 300 mg/L.

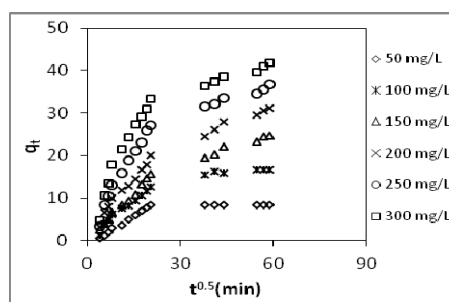


Fig. 9. Intraparticle diffusion kinetics of safranine adsorption onto the treated sample at different initial dye concentrations.

The mechanism of adsorption is considered to involve three steps and the intraparticle diffusion model was used in order to determine the rate-limiting step of adsorption process. The first part of plot (0 - 10 min^{1/2}) was attributed to the diffusion of safranin to the outer surface of adsorbent. The second part of plot (10 - 30 min^{1/2}) can be considered as the gradual adsorption of safranin into the particle interior as seen in Fig. 10.

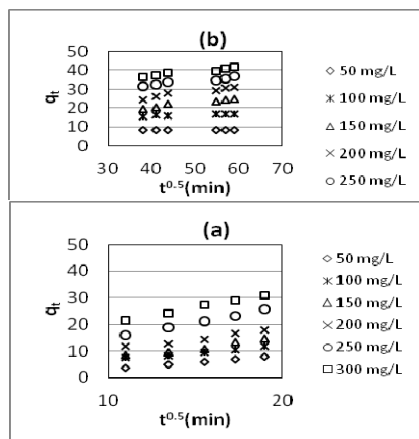


Fig. 10. Two steps of intraparticle diffusion (a) the gradual adsorption of safranin into the particle interior, (b) the final equilibrium stage.

TABLE V: DIFFUSION RATE CONSTANT AND CORRELATION COEFFICIENT, R^2 , ONTO TREATED AND UNTREATED SAMPLES

Untreated			
C_0 (mg/L)	k_i (mg/g min ^{0.5})	I (mg/g)	R^2
50	0.114	1.138	0.808
100	0.223	2.455	0.911
150	0.311	2.65	0.936
200	0.329	5.156	0.908
250	0.401	5.708	0.91
300	0.425	7.132	0.889
Treated			
C_0 (mg/L)	k_i (mg/g min ^{0.5})	I (mg/g)	R^2
50	0.138	2.831	0.636
100	0.24	4.348	0.931
150	0.374	4.604	0.848
200	0.45	6.579	0.934
250	0.496	10.36	0.846
300	0.523	14.44	0.791

The intraparticle diffusion leads to slow down due to occupation of the active sites by safranin molecules; therefore, the third part of adsorption process (30 - 90 min^{1/2}) was assigned to the final equilibrium stage. The deviation of the straight lines from the origin indicates that film diffusion and intra-particle diffusion occurred simultaneously. The intercept and diffusion rate constant of all concentrations are listed in Table. 5. The intercept values increased in ranging 1.138 - 7.132 mg/g and 2.831 - 14.44 mg/g for the untreated and treated samples with increasing the initial concentrations from 50 - 300 mg/L and indicating the high concentrations encouraged the boundary layer diffusion effect.

IV. CONCLUSIONS

The present study shows that the alkali-treated mango seed integument can be considered as a low-cost adsorbent for the removal of safranin from aqueous solution. Batch

experiments were carried out in order to study equilibrium isotherms, kinetics models and the parameters such as the pH of the solution, determination of pH_{pzc} and the surface chemistry. The alkali treatment resulted in an increase in the phenolic functional groups by three times. Also, the acidity of the adsorbent's surface increased from (0.375 mmol/g) to (0.660 mmol/g) after NaOH treatment. By considering the good agreement between $q_{e,cal}$ and $q_{e,exp}$, the kinetic data were fitted to pseudo second-order isotherm adsorption model.

ACKNOWLEDGMENTS

The authors would like to gratefully acknowledge Azad University, Shahreza Branch for the financial support of this work.

REFERENCES

- [1] O. Gercel, H. F. Gercel, A.S. Koparal, U. B. Oğutveren, "Removal of disperse dye from aqueous solution by novel adsorbent prepared from biomass plant material," *J. Hazardous. Mater.*, vol. 160, pp. 668-674, 2008.
- [2] B. E. Barragan, C. Costa, and M. C. Marquez, "Biodegradation of azodyes by bacteria inoculated on solid media," *Dyes Pigments*, vol. 75, pp. 73-81, 2007.
- [3] S. Wang, "A comparative study of Fenton and Fenton-like reaction kinetics in decolourisation of wastewater," *Dyes Pigments*, vol. 76, pp. 714-720, 2008.
- [4] Q. Y. Yue, B. Y. Gao, Y. Wang, H. Zhang, X. Sun, S. G. Wang, and R. R. Gu, "Synthesis of polyamine flocculants and their potential use in treating dye wastewater," *J. Hazard. Mater.*, vol. 152, pp. 221-227, 2008.
- [5] Y. Z. Jin, Y. F. Zhang, and W. Li, "Micro-electrolysis technology for industrial wastewater treatment," vol. 15, pp. 334-338, 2003.
- [6] N. P. Cheremisinoff, "Handbook of Water and Wastewater Treatment Technologies. Butterworth-Heinemann," Boston, 2002.
- [7] T. H. Kim, C. Park, J. M. Yang, and S. Kim, "Comparison of disperse and reactive dye removals by chemical coagulation and Fenton oxidation," *J. Hazard. Mater.*, vol. 112, pp. 95-103, 2004.
- [8] Z. Liu, Y. He, F. L., and Y. Liu, "Photocatalytic Treatment of RDX Wastewater with Nano-Sized Titanium Dioxide," *Envir. Sci. Pollut. Res.*, vol. 13, pp. 328-332, 2006.
- [9] C. H. Weng, Y. C. Sharma, and S. H. Chu, "Adsorption of Cr (VI) from aqueous solutions by spent activated clay," *J. Hazardous Mater.*, vol. 155, pp. 65-75, 2008.
- [10] P. K. Malik, "Use of activated carbons prepared from sawdust and rice-husk for adsorption of acid dyes: A case study of acid yellow 36," *Dyes Pigments*, vol. 56, pp. 239-249, 2003.
- [11] F. Ferrero, "Dye removal by low cost adsorbents: hazelnut shells in comparison with wood sawdust," *J Hazard Mater*, vol. 142, pp. 144-152, 2007.
- [12] M. Ozacar, A. Engil, "Adsorption of metal complex dyes from aqueous solutions by pine sawdust," *Bioresour. Technol.*, vol. 96, pp. 791-795, 2005.
- [13] G. Annadurai, R. S. Juang, D.J. Lee, "Use of cellulose-based wastes for adsorption of dyes from aqueous solutions," *J. Hazard. Mater.*, vol. 92, pp. 263-274, 2002.
- [14] J. F. Osma, V. Saravia, J. L. T. Herrera, and S. R. Couto, "Sunflower seed shells: a novel and effective low-cost adsorbent for the removal of the diazo dye Reactive Black 5 from aqueous solutions," *J. Hazard. Mater.*, vol. 147, pp. 900-905, 2007.
- [15] M. Valix, W. H. Cheung, and G. McKay, "Preparation of activated carbon using low temperature carbonisation and physical activation of high ash raw bagasse for acid dye adsorption," *Chemosphere*, vol. 56, pp. 493-501, 2004.
- [16] Y.J. Tham, P. A. Latif, A. M. Abdullah, A. S. Devi, and Y. H. T. Yap, "Performances of toluene removal by activated carbon derived from durian shell," *Bioresour. Technol.*, In press, 2010.
- [17] K. Vasanth and A. Kumara, "Removal of methylene blue by mango seed kernel powder," *Biochem. Eng. J.*, vol. 27, pp. 83-93, 2005.
- [18] L. S. Balistreri and J. W. Murray, "The surface chemistry of goethite (FeOOH) in major ion seawater," *Am. J. Sci.*, vol. 281, pp. 788-806, 1981.
- [19] G. Crini, H. N. Peindy, F. Gilbert, and C. Robert, "Removal of c.i. basic green 4 (malachite green) from aqueous solutions by adsorption

- using cyclodextrin- based adsorbent: kinetic and equilibrium studies,” *Separation and Purification Technology*, vol. 53, pp. 97-110, 2007.
- [20] S. L. Goertzen, K. D. Theriault, A. M. Oickle, A. C. Tarasuk, and H. A. Andreas, “Standardization of the Boehm titration. Part I. CO₂ expulsion and endpoint determination,” *Carbon*, vol. 48, pp. 1252-1261, 2010.
- [21] A. Dabrowski, P. Podkoscielny, Z. Hubicki, and M. Barczak, “Adsorption of phenolic compounds by activated carbon - a critical review,” *Chemosphere*, vol. 58, pp. 1049-70, 2005.
- [22] S. F. Dyke, A. J. Floyd, M. Sainsbury, and R. S. Theobald, “Organic Spectroscopy: An Introduction,” 2nd ed. Longman, New York, 1981, pp. 58-88.
- [23] C. S. Meireles, G. R. Filho, M. F. Ferreira, D. A. Cerqueira, R. M. N. Assunção, E. A. M. Ribeiro, and P. P. M. Zeni, “Characterization of asymmetric membranes of cellulose acetate from biomass: Newspaper and mango seed,” *Carbohydrate Polymers*, vol. 80, pp. 954-961, 2010.
- [24] S. N. Guha and J. P. Mittal, “Pulse radiolysis study of one-electron reduction of safranin T,” *J. Chem. Soc., Faraday Trans*, vol. 93, 1997.
- [25] S. Sohn and D. Kim, “Modification of Langmuir isotherm in solution systems—definition and utilization of concentration dependent factor,” *Chemosphere*, vol. 58, pp. 115-123, 2005.
- [26] I. A. W. Tan, A. L. Ahmad, and B. H. Hameed, “Enhancement of basic dye adsorption uptake from aqueous solutions using chemically modified oil palm shell activated carbon,” *Colloids and Surfaces A: Physicochem. Eng. Aspects*, vol. 318, pp. 88-96, 2008.
- [27] I. D. Mall, V. C. Srivastava, G. V. A. Kumar, and I. M. Mishra, “Characterization and utilization of mesoporous fertilizer plant waste carbon for adsorptive removal of dyes from aqueous solution,” *Colloids and Surfaces A: Physicochem. Eng. Aspects*, vol. 278, pp. 175-187, 2006.
- [28] S. Lagergren, “About the theory of so called adsorption of soluble substances,” vol. 24, pp. 1-39, 1898.
- [29] Y. S. Ho, J. C. Y. Ng, and G. McKay, “Kinetics of pollutants sorption by biosorbents: review,” *Sep. Purif. Methods*, vol. 29, pp. 189-232, 2000.
- [30] T. W. Weber and R. K. Chakravorti, “Pore and solid diffusion models for fixed bed adsorbers,” *A. I. Ch. E. J.*, vol. 20, pp. 228-238, 1974.